# Phase-Locking Josephson Junctions Arrays

M.Cirillo
Universita' di Roma Tor Vergata
(Roma II)

This publication is based (partly) on the presentations made at the European Research Conference (EURESCO) on "Future Perspectives of Superconducting Josephson Devices: Euroconference on Physics and Application of Multi-Junction Superconducting Josephson Devices, Acquafredda di Maratea, Italy, 1-6 July 2000, organised by the European Science Foundation and supported by the EuropeanCommission, Research DG, Human Potential Programme, High-Level Scientific Conferences, Contract HPCFCT-1999-00135. This information is the sole responsibility of the author(s) and does not reflect the ESF or Community's opinion.The ESF and the Community are not responsible for any use that might be made of data appearing in this publication.

# Phase-Locking Josephson Junctions Arrays

M. Cirillo

Dipartimento di Fisica and Unità INFM

Università di Roma "Tor Vergata", I-00133 Roma, Italy

G. Rotoli

Dipartimento di Energetica and Unità INFM

Università di L'Aquila, I-67040 L'Aquila, Italy

F. Mueller, J. Niemeyer, and R. Poepel

Physikalisch-Technische Bundesanstalt

Bundesallee 100, D-38116 Braunschweig, Germany

## Abstract

We demonstrate that a large area Josephson junction oscillating in the fluxon oscillator mode can be synchronized to other large junctions and simultaneously pump , by emitted radiation, a small area junction. We study the synchronization of the oscillations of the long junctions as a function of relevant experimental parameters such as bias current and stripline coupling characteristics. Experimental results obtained on coupled series arrays of Josephson junctions designed on the basis of our calculations are presented. We have fabricated coupled arrays containing each up to 1500 junctions in order to estimate the usefulness of our calculations for voltage standard devices.

PACS numbers: 74.50.+r, 74.40.+k

## I. INTRODUCTION

The reliable fabrication technology of Josephson junctions based on all refractory materials has allowed realization of several successful integrated superconducting circuits and devices. A new limit has been established, using a multiwasher device, for the sensitivity of dc-SQUIDs [1] and reliable voltage standard devices are nowadays used for calibrations up to 10V [2] . A fully integrated receiver system is presently being developed [3] : this device includes a long Josephson junction (LJJ) biased on Fiske and Eck steps [4] as a pumping device of the SIS mixer element .

Along with the success achieved in superconducting devices the well established fabrication process has opened new perspectives in the study of the physics of complex tunnel junction-based systems such as multi-stacked junctions [5–7], large planar arrays [8], macroscopic evidence of quantum levels [9] and complex bidimensional dynamics [10].

Very recently, interesting evidence of coherence and phase-locking in two-dimensional arrays based on trilayer Josephson junctions has been reported by Barbara et. al [8]. These experiments have confirmed that the problem of the coherence of nonlinear systems is intriguing, stimulating, and potentially very useful for applications. Indeed, several publications were devoted to the study of phase-locking phenomena in Josephson systems in the past two decades; beside the interest for the practical realization of Josephson voltage standards [11], work was also devoted to the study of the locking between planar distributed oscillators [12–16].

In the present paper we investigate by numerical simulations and experiments phase-locking phenomena in hybrid Josephson junctions systems; the systems investigated are hybrid in the sense that they contain both long junctions and small area Josephson junctions (SJJ). We investigate the ranges of stability of the phase-locking between a LJJ oscillator and a small junction and the possibility of phase-locking an array of LJJ oscillators to an array SJJ ; we also report on experiments that have been thought and performed on the basis of our calculations. We recall here that the physical dimensions of Josephson tunnel junctions

are considered "long" or "short" depending on their size relative to the penetration depth $\lambda_j = \sqrt{\frac{\Phi_0}{2\pi \mathcal{I} \mathsf{L}}}$ where $\Phi_0 = 2.07 \times 10^{-15} Wb$ is the flux quantum; $\mathcal{I}$ and $\mathsf{L}$ represent respectively the supercurrent density and inductance per unit length of the junctions.

In the next section we describe the capacitive coupling model at the basis of our simulations and present the results obtained for the long Josephson oscillators coupled to small junctions. In sect. III we show the numerical results obtained for the coupling of two arrays ; in sect. IV we present experimental data that have been obtained on real Josephson junctions arrays. In sect. V we conclude the paper discussing the possible impact of our results on voltage standard research and superconducting electronics.

## II. THE MODEL

The model that we intend to investigate consists in its simplest form of two long Josephson junction coupled each at one end to a small area junction which is the system shown in Fig. 1. Before analyzing the full circuit equations for this model we will go through two preliminary steps. Let us consider first the circuit equations obtained from this figure considering only one LJJ coupled via the capacitor $C_1$ to the SJJ above it and neglect the rest of the circuit : shorting as shown by the dashed vertical lines the Kirchoff laws give the equations that follow

$$C_1 \left( \dot{v}_s - \dot{v}_L \right) = J_s \tag{1}$$

$$C_1 \left( \dot{v}_L - \dot{v}_s \right) = J_L \tag{2}$$

where $C_1$ is the coupling capacitor between small and long junctions; $v_s$ and $v_L$ are, respectively, the voltages of small and long junction (at one end point); $J_s$ and $J_L$ are currents from Josephson elements which can be written as:

$$J_s = -C_s \dot{v}_s - G_s v_s - I_s \sin \varphi_s + I_s^b \tag{3}$$

$$J_L = -\mathcal{C}(\Delta x/2)\dot{v}_L - \mathcal{G}(\Delta x/2) v_L - \mathcal{I}(\Delta x/2) \sin \varphi_L + \tag{4}$$
$$+ \mathcal{I}^b(\Delta x/2) + \frac{\Phi_0}{2\pi \mathsf{L}} \frac{\partial^2 \varphi_L}{\partial x^2} (\Delta x/2)$$

where , $C_s, G_s$,and $I_s$ are respectively the capacitance, the conductance and Josephson supercurrent of the small junction, while $\mathcal{C}$ and $\mathcal{G}$ are respectively the capacitance and the conductance per unit length. Finally $\Delta x$ is the length of the last element of long junction and $I_s^b$ and $\mathcal{I}^b$ are, respectively, the bias current of small junction and bias current per unit length of long junction (normalized to the maximum Josephson supercurrent). In this paper we will often set $\gamma \equiv I_s^b$ for typhographycal convenience.

The system of differential equations (1)-(4) has been integrated, after discretizing the long Josephson junction in $N$ sections, by a Bulirsh-Stoer routine. We choosed for the long junction a normalized length $l = 3$ with $N = 60$ sections. We tested that the results were not dependent upon $N$ making runs with different values of $N$. We note that, for simplicity, we assumed the bias current uniformley distributed inside the long junctions. However, as far as fluxon oscillations are concerned, for the lengths and the loss parameter that we will consider, there is not much difference in the fluxon dynamics between overlap (uniform) or inline (boundary) bias current injection. Thus, the internal dynamics of the LJJ was accounted for by an equation similar to eq. 4 with the left hand side set to zero. At the uncoupled ends of the LJJs we imposed open circuit boundary conditions.

In the first set of simulations in which we only coupled a single long junction to a single small junction this latter had a normalized length $l_s = 0.05$ corresponding to one section of long junction model. Current densities are assumed equal in the long and small junction and in all simulations the time is normalized to the plasma frequency $\omega_j = \sqrt{\frac{2\pi\mathcal{I}}{\Phi_0\mathcal{C}}}$. In order to avoid pumping of the small junction below its plasma frequency its capacitance was chosen slightly larger than that of a unit section of the long junction. For both junctions we fixed a loss parameter $\alpha = \frac{1}{\sqrt{\beta_c}} = G_s\sqrt{\frac{\Phi_0}{2\pi C_s I_s}} = 0.025$ .

The results of the integrations were analyzed in terms of voltage and phase versus time plots, but we believe that the clearest way to display the results is the plot of the current-voltage characteristics of the junctions. The basic coupling scheme described by the system (1)-(4) was investigated in ref. 17 and it was found that the relevant parameter for the capacitive loading is the normalized quantity $\zeta = C_1/\mathcal{C}\lambda_j$. In Fig. 2a we show the result

of an integration obtained fixing all the parameters of the coupled system as described in the previous paragraph and the coupling parameter $\zeta = 0.008$ . Under these conditions the single fluxon shuttling oscillations in the long junction generated a "natural" oscillation frequency which gave rise to a voltage $V_s \cong 2$ and very stable zero-field steps (ZFS) [12,13] in the current-voltage characteristics. In the Fig. 2a we report part of the current-voltage characteristic of the "small" junction where we can see Shapiro steps in the current-voltage characteristics obtained for a dc bias point of the long junction model determined by $\mathcal{I}^b = 0.25$. The phase-locking between the junctions is very stable and the first Shapiro steps (which crosses the zero current axis) has an amplitude which goes up to 15% of the Josephson critical current.

In Fig. 2b we show the obtained amplitude of the first Shapiro step of the small junction obtained sweeping the coupling parameter from zero up to 0.016 for three different values of the dc bias current of the long junction which are, respectively 0.15, 0.3, and 0.45 for circles,squares, and triangles; all the other parameters were like in Fig. 2a. The figure shows that for the higher values of the coupling parameter the amplitude of the step goes up to 30% of the maximum Josephson supercurrent and that the amplitude of the step is not critically dependent upon the value of the bias current in the long junction. This configuration and such step amplitudes would be enough to provide a stable dc bias point on the Shapiro step for voltage standard oriented applications. Note that the points on the zero-voltage axis in Fig. 2a represent the Josephson current that in this case was depressed of 10% of its maximum value.

## III. COUPLED ARRAYS

We analyze now the circuit shown in Fig. 1 in two situations more complex than that reported in the previous section. We will first consider the circuit obtained removing the vertical shorting path (dashed line) in the LJJs series connection and adding a shorting path as shown by the horizontal dashed line. Successively we will consider the dynamics of the whole circuit (with no shorting paths) ; in the first case investigated here two coupled long

junctions are pumping by means of the capacitors $C_1$ and $C_2$ a single small junction and the equations that we integrate are:

$$C_1\left(\dot{v}_{L1}-\dot{v}_s\right)+C_3\left(\dot{v}_{L1}-\dot{v}_2\right)\;=J_{L1} \tag{5}$$

$$C_3\left(\dot{v}_{L2}-\dot{v}_{L1}\right)+C_2\left(\dot{v}_{L2}-\dot{v}_s\right)\;=J_{L2} \tag{6}$$

$$C_1\left(\dot{v}_s-\dot{v}_{L1}\right)+C_2\left(\dot{v}_s-\dot{v}_{L2}\right)\;=J_s \tag{7}$$

Here again $J_s$, $J_{L1}$ and $J_{L2}$ are currents from Josephson elements that can be written as in eqs. (3) and (4) and $C_3$ is the coupling capacitor between two long junctions. In the simulations we have neglected the effect of the inductors connecting the two long junctions : the effect of these inductors, from the point of view of the modelling is to provide a series dc connection between the junctions. At high frequency, in practical experimental situations, we have estimated that the values of the inductances connecting the junctions are so high that most of the rf current goes through the capacitor. We started the integration in the two LJJs with initial data generating single flux-quanta oscillations in both the junctions with arbitrary position. The same bias current was feeding both junctions ; this biasing condition can model a series dc-bias which, as we shall see, is a good approximation of the experimental conditions that we are going to model.

The results obtained by coupling two LJJs with normalized lengths different of 3% to a single small junction are shown in Fig. 3a ; the numerical integration in this case was obtained for the same set of parameters of Fig. 2a with the coupling between the long junctions determined by $\zeta = 0.075$ and identical coupling between each long junction and the small one, i.e., $C_1 = C_2$ (and $\zeta = 0.008$). Here, as before, the points on the zero-voltage axis represent the Josephson current that was depressed in this case of about 25% of its maximum value. We can see that, for the same value of the coupling parameter (between the long and the short junction) the amplitude of the step is larger than in the previous case in which a single long junction is acting as a pumping element.

Although a part of the radiation emitted by a single LJJ is injected in the other long junction and provides the phase-locking of the oscillations, there is an evident increase

of power feeding the small junction that we estimate to be of the order of 66% at the fundamental frequency of the first Shapiro step. Thus, we conclude that the amplitude of the first phase-locked Shapiro step can be increased by pumping the small junction with two synchronized long junctions. It is worth noting that the phase-locking of the two LJJs with different lengths produces a single frequency output : we verified this conditions within the limits of the numerical uncertainty. In Fig. 3b we show in this case the dependence of the amplitude of the first Shapiro step upon the coupling parameter : the value of the bias current of the LJJs for this figure was $\mathcal{I}^b = 0.25$.

Let us consider now the whole system shown in Fig. 1 consisting of two series-connected small junctions and two series-connected long junctions coupled by capacitors. The equations that we have integrated in this case are:

$$C_3 \left(\dot{v}_{L1} - \dot{v}_{L2}\right) + C_1 \left(\dot{v}_{L1} - \dot{v}_{s1}\right) = J_{L1} \tag{8}$$

$$C_3 \left(\dot{v}_{L2} - \dot{v}_{L1}\right) + C_2 \left(\dot{v}_{L2} - \dot{v}_{s2}\right) = J_{L2} \tag{9}$$

$$C_1 \left(\dot{v}_{s1} - \dot{v}_{L1}\right) = J_{s1} \tag{10}$$

$$C_2 \left(\dot{v}_{s2} - \dot{v}_{L2}\right) = J_{s2} \tag{11}$$

Here, as in the system of eqs. (5)-(7) we have neglected the effect of the inductors connecting the two long junctions and the two small junctions ; $J_{s1}, J_{s2}$, $J_{L1}$ and $J_{L2}$ can be written as in eqs. (3) and (4). In Fig. 4 , as a result of the series connection the voltages of the small area junctions are summed up and therefore we see two zero crossing steps which correspond to the Shapiro step appearing at the fundamental frequency of the pumping process. Even for this figure the coupling between the long junctions was characterized by $\zeta = 0.075$ and the coupling between long and small junctions by $C_1 = C_2$ (and $\zeta = 0.008$). As in the previous cases, the voltage output was "monochromatic" within the errors imposed by the numerical integration routine, meaning that the two zero-crossing Shapiro steps of Fig. 4 can be viewed as two steps of a single junction. Here we have imposed a difference of 3% between the normalized length of the two long junctions.

In Fig. 5 instead we show the dependence of Shapiro steps at the fundamental pumping

frequency upon the coupling parameter between long and short junctions for three percentages of difference in length of the junctions : in the figure squares and full circles show the different height of the Shapiro steps at the fundamental frequency in the two small junctions. The value of the coupling parameter between the long junctions increases from a) to c). In particular, we have $\zeta = 0.025$, $\zeta = 0.075$,and $\zeta = 0.15$ resp. for a), b), and c) ; the results of Fig. 4 and Fig. 5 are quite similar to those of Fig. 3 meaning that the simultaneous rf biasing of the two small junctions is very stable and a stable phase-locking to the LJJs signal is generated. We also performed simulations in which slightly different parameters for the two small junctions which did not modify significantly the features that we have described so far.

## IV. EXPERIMENTS

A system composed by one LJJ coupled capacitively to a single SJJ (1+1 case) has already been experimentally investigated [17] ; measurements on real Josephson junctions were also reported for the (2+1) system, in which two LJJs oscillators are coupled to one SJJ [18] . In both cases good agreement was found between experimental data and the predictions of the theoretical analysis and simulations; in the (2+1) case in particular, the experiments confirmed an increase of the detected radiation when pumping the SJJ with two coherent oscillators, just like we found in the simulations. However, both in ref. 17 and ref. 18 the coupling capacitor was obtained adding extra layers to the ones required for the growth of the junctions ; the extension of that fabrication technique (and coupling concept) to large coupled arrays, an important practical counterpart of our work, would not be easy.

The main problem with the experimental realization of large coupled arrays employing as a basic building block the system studied in the previous section is topological. Since we wanted to keep the configuration of our final layout planar and the fabrication of the circuit compatible with the existing Nb-Al/AlOx-Nb trilayer technologies, the design of the system closer to our theoretical modelling was not straightforward. As far as the coupling between the long junctions is concerned, we know that having two ends of the long junctions facing

each other may provide by itself a good capacitive connection, very effective for phase-locking [12]. The topological constraint arises because we must couple capacitively two series arrays which should be decoupled from the dc point of view without adding extra layers to the trilayer junction fabrication technology. However, since in series connection of junctions we can have only two junctions on the same trilayer island, the basic LJJ building block of our experimental system will be close to the one investigated numerically, i. e. two coupled long junctions.

The samples that we produced were obtained according to a standard PTB Nb trilayer processing [2]. The junctions had a critical current density of 1400 $A/cm^2$ and a Josephson penetration depth $\lambda_j = 10\mu m$ . Also, we recall that in this technology the specific capacitance of the tunnel junctions is $C_s = 3\mu F/cm^2$. In Fig. 6a we show a detail of the final product of the fabrication process : in the photograph the position of long and short junctions is indicated by the darker areas. It is worth noting that we sputtered on the back of the Si wafer a layer of Nb with the intention of using it as a groundplane. In the photograph we just see two basic units of our system, i.e. a Nb island with two small junctions on the top and another with two long junctions on the top.

The coupling (and the values of the parameter $\zeta$) between two long junctions on the same Nb island was calculated assuming that the capacitance connecting the LJJs is due to the gap in the striplines. Since the gap separating the two top electrodes of the long junctions is relatively small (there is only a 10 $\mu m$ distance between the top electrodes), we estimate, using the typical junction parameters of Nb trilayer technology and the matrix inversion method [19], a $C_0 \cong 26\ fF$ and therefore a coupling factor $\zeta = 0.045$. We note that, due to the fact that the trilayer is grown over an oxidized Si substrate which has a groundplane on the back, there exists also a capacitive coupling between the base Nb islands due to the capacitor formed between the top connecting electrode, the Si substrate, and the ground plane. The capacitance of this element, however, is of the order of 0.1 $fF$ which gives $\zeta \cong 10^{-4}$ ; thus, the coupling between the long junctions on different islands is neglegible

with respect to the contribution calculated for the junctions on the same island. However, even if it is small, a coupling between the islands containing each two junctions exists.

In order to couple capacitively the two arrays of long and small junctions we adopted the following strategy . we fabricated two arrays of junctions that formed each a meander-like line: the two meanders formed respectively by the series arrays of long and small junctions arrays fit each other as shown in Fig. 6b. In these conditions we assume that an interdigital capacitive coupling exists between the two series arrays and that for this coupling the capacitance/unit length is regulated by the equation [20]

$$C_{ul} = (\frac{\epsilon_r + 1}{W})L[(n-3)A_1 + A_2]pF/in$$

where $n$ is the number of fingers of the interdigital capacitor, $L$ their length in inches, $W$ the total length of the capacitor in inches, and $A_1$ and $A_2$ are two variables depending on the thickness of the substrate and on the spacing between the fingers. In our case the dielectric layer is represented by the 0.375 $mm$ thick Si substrate (for Si we assume $\epsilon_r = 11.4$ at 4.2K [21]), the length of the fingers is $L = 2.2$ $mm$ and their spacing is of the order of 20 $\mu m$ . Thus, the coupling is caracterized by a capacitance/unit length given by $C_{ul} = (\frac{12.4}{W})L[(n-3)0.1 + 0.23]$ $pF/in$. This equation is expected to hold only if the substrate thickness $T > (W/n)$ where $W$ is the total length of the interdigital structure : in our case, since $T = 0.375$ $\mu m$ , if the length of a unit cell is of the order of 64 $\mu m$ (to form a unit cell we need a minimal number three fingers) , this condition can be expected to hold even if $n = 3$ . The capacitance of the unit cell of our interdigital structure [20] has been evaluated in our case with two coupled arrays constituted each of 64 junctions. In this case we get, for $W = 64$ $\mu m$ and $n = 3$ a coupling capacitor of 0.24 $pF$.

It is worth noting that in our interdigital capacitive modelling we evaluate the overall capacitance coupling the two ports (which are the long and short junction array). Since radiation is distributed all over the stripline of one port (the radiation emitted from the long junctions), we assume that each small junction of the "detector" port will receive the

amount of radiation coupled capacitively by the interdigital structure. At the same time, however, each basic cell of the long junction array shall be loaded by the same capacitor (see the circuit model shown in Fig. 1 of ref. 19 ) because all the junctions of the two arrays are faced in parallel to ground; more precisely, we have all the junctions capacitances in series to ground with the capacitance of the striplines. We neglect the effect of the junctions capacitances since these are much larger than that of the striplines. The basic limit of our assumptions is the fact that our fingers are "empty", however, considered the frequencies at which our samples are operating (only up to 90 $GHz$) and considered that the empty slot in our fingers are only few microns wide, we think that the interdigital capacitive coupling described above is a first rough but reasonable approximation. In terms of this modelling the problem of loading the basic unit of the arrays can be reduced to the (2+2) junction system analyzed in the simulatins because all the long junctions of the array are loaded in paralled by the interdigital capacitor.

The experimental results that we obtained with the arrays were consistent with the predictions of this model. From the model we can expect that the coupling will be better for arrays having an increasing number of fingers ($n$) . We can calculate that for $n = 3$ the coupling parameter between two adjacent fingers (i. e. between one double row of long junctions and one double row of small junctions) is $\zeta = 0.15$ which takes us in a region [17] where the reflection of fluxons at the ends of the long junctions and the coupling of electromagnetic radiation to other junctions is just below a threshold value for absorption. This would be a very privileged region in terms of transfering power from a fluxon oscillator to other junctions [17] and we would expect, within the limits of our modeling, radiation-coupling effects. Naturally, increasing the number of fingers we expect more radiation being coupled.

We fabricated several samples and we show in Fig. 7, Fig. 8, and Fig. 9 typical results. Fig. 7 shows oscillator on-oscillator off current-voltage characteristics of a 64 junctions SJJ array coupled to an array of 64 LJJs (a unit cell in terms of our interdigital capacitor

modelling). In order to obtain the emission of radiation we biased the LJJ array with a current of 600 $\mu A$ at a voltage of 32 $mV$ and . For this sample the the physical extended dimension of the long junctions was $50\mu m$ and the ZFS appeared at asymptotic voltages , in each junction, of 334 $\mu V$ ; thus, at the voltage of 32 $mV$ we were biased roughly on the 96th ZFS of the long junctions array which makes sense because we had two and sometimes three ZFS for a single junction. We note, however, that in this case the observed suppression of the Josephson current of about 40% . This result is consistent with the numerical simulations because in the experiments we have a coupling parameter $\zeta = 0.15$ which is larger than that $\zeta = 0.008$ value of the simulations which allowed a maximum 25% suppression of the Josephson current.

A result similar to that shown in Fig. 7 was also obtained, see Fig. 8, coupling only eight oscillator junctions to eight detector junctions which were just placed along two parallel lines. In this case the length of the long junctions and the asymptotic voltages of the ZFSs were the same as for Fig. 7 ; the bias point of the oscillator array was defined by a current of 600 $\mu A$ and a voltage of 4.5 $mV$ and therefore we were biased on the $13th$ ZFS of the array. We see that the relative suppression of the critical currents of the detector array is now of the order of 25% , a result that is not very different from the previous one. As one can expect [19,20], the coupling provided between the arrays of a unit cell of our interdigital capacitor is of the same order of magnitude of that provided by the coupling of the two microstrips formed by the series arrays. The situation is very different instead when we increase the number of fingers.

In Fig. 9 indeed we show evidence that our coupling scheme is very effective in transfering power between the two arrays increasing the number of fingers $n$ : In this figure we see a full depression of the Josephson currents of the array of small junctions. For this figure we measured an array of 1564 junctions that was coupled to an array of 1564 LJJs and the number of nested fingers was $n = 47$ for which we estimate a coupling capacitor between the two arrays of the order of 4.9 $pF$ and a coupling factor $\zeta = 3$ . We note that in this

case we observed the same coupling of power independently upon the number of biased long junctions : we varied the bias current on the zero-field steps of the oscillator array in a way that the corresponding voltage would range from few tens up to few hundreds millivolts. This observation leads us to conclude that the coupled power was not a function of the number of biased oscillators but just an effect of the geometrical configuration. The same effect shown in Fig. 9 was measured in several other samples. For the pictures of Fig. 9 we had an oscillator bias current of 380 $\mu A$ and relative voltage of 80 $mV$ meaning that, since the length of the junctions was the same as before (Fig. 7 and Fig. 8), we were biased on the 240 $th$ ZFS of the array.

The fact that we observe a full depression of the Josephson current for a coupling factor $\zeta \simeq 3$ is still a factor of consistency between experiments and numerical simulations because in the simulations we always found that increasing the coupling parameter more radiation was transmitted from the long to the short junctions. However, such an high coupling factor would mean an excessive loading of the junctions [17] and the disappearance of the soliton oscillations. This result implies that the modelling in terms of interdigital capacitive coupling needs refinements because in the experiments we always observed very stable zero-field steps. It is likely that the overall capacitor connecting the two arrays has a value lower than the one we estimated by the interdigital capacitive modelling. Also, as one can see in Fig. (7-9) our arrays had a somewhat high subgap current and it is likely that the coupled em power in this voltage region is mostly dissipated resistively. Thus, it was difficult in our case to observe stable Shapiro steps in the subgap regions. These steps were visible at the frequencies expected from the bias point on the oscillator arrays but had a current amplitude of few microamperes. At present we are fabricating samples that should enable us to improve the quality of the current-voltage characteristics of the junctions, to perform more systematic tests of the interdigital capacitive coupling between the arrays, and to obtain convincing evidence of the overall coherence of the large number of oscillators.

## V. CONCLUSIONS

We have shown numerically that a complicated nonlinear system represented by a coupled array of two long and two short Josephson exhibits remarkable phase-locking properties. The simulations have shown that the power emitted by the large junctions can be used both to synchronize them and to pump small area junctions. From the numerical results we have also seen that the coherent oscillation gives rise to an increase of the emitted radiation, a phenomenon that has been observed even in the experiments. The stability of the phase-locking in the numerical simulations investigated for practical ranges of disuniformities between the junctions is such that applications of our results in the field of metrology and millimeter-wave electronics can be thought. We have reported experimental evidence that the effect found in the simulations due to a capacitive coupling can be observed in arrays shaped in a meander line and nested in an interdigital way. The experiments have shown that radiation can be transmitted from one large oscillator array to a large detector array without affecting the stability of the oscillators and that the coupled em power it is not dependent on the bias voltage of the oscillators. In these arrays the basic building block is just represented by the system investigated in the simulations

Our coupling scheme required, in terms of space, for the two arrays having each 1564 junctions, less than 2 $mm^2$ (excluding the contact pads). This number of junctions is typical for a one volt standard array chip. Also, the extension to 10V chips can be easily predicted to occupy less space than the finline antenna of the samples nowadays used for standard maintenance; therefore frequency stabilizer circuits and counters could easily be integrated along with the coupled arrays. The major advantage of our coupling scheme for the point of view of the rf-biasing of large voltage standard arrays (both classical and programmable) is the fact that the em power is distributed more uniformly all over the junctions. This characteristic might turn out to be especially useful for the new SINIS voltage standard technology [22] for which a relatively low amount of microwave power is required : it would not be very difficult to substitute our small junctions array with a SINIS one. Beside these encouraging perspectives for voltage standard purposes we believe that our radiation transfer

scheme could lends itself to other applications in superconducting electronics.

## ACKNOWLEDGMENT

This work was partially supported by the MURST (Italy) through a COFIN98 project.

The paper is dedicated to the memory of our colleague Ralf Poepel whose premature fading represented an hardly recoverable loss for the research on voltage standard devices.

# REFERENCES


[1] P. Carelli, M. G. Castellano, G. Torrioli, and R. Leoni, Appl. Phys. Lett. **72**, 115 (1998).

[2] J. Kohlman, F. Mueller, P. Gutman, R. Poepel, L. Grimm, F.-W. Duehnschede, W. Meier, and J. Niemeyer, IEEE Trans. Appl. Superc. **7**, 3411 (1997).

[3] V. P. Koshelets, A. V. Shchukin, S. V. Shitov, and L. V. Filippenko, IEEE Trans. Appl. Superconductivity **3**, 2524 (1993).

[4] M. Cirillo, N. Grønbech-Jensen, M. R. Samuelsen, M. Salerno, and G. Verona Rinati, Phys. Rev. **B58**, 12377 (1998).

[5] S. Sakai, A. V. Ustinov, H. Kohlstedt, A. Petraglia, and N. F. Pedersen, Phys. Rev. **B50**, 12905 (1994).

[6] N. Grønbech-Jensen, J. A. Blackburn, and M. R. Samuelsen, Phys. Rev. **B53**, 12364 (1996).

[7] N. F. Pedersen and S. Sakai, Phys. Rev. **B58**, 2820 (1998).

[8] P. Barbara, A. B. Cawthorne, S. V. Shitov, and C. J. Lobb, Phys. Rev. Lett. **82**, 1963 (1999).

[9] P. Silvestrini, V. G. Palmieri, B. Ruggiero, and M. Russo, Phys. Rev. Lett. **79**, 3046 (1997).

[10] C. Nappi, R. Cristiano, and M. P. Lisitskii, Phys. Rev. **B58**, 11685 (1998).

[11] R. L. Kautz, Rep. Prog. Phys. **59**, 935 (1996).

[12] M. Cirillo and F. L. Lloyd, J. Appl. Phys. **61**, 2581 (1987).

[13] R. Monaco, S. Pagano, and G. Costabile, Phys. Lett.**A131**, 122 (1988).

[14] G. Reinisch, J. C. Fernandez, N. Flytzanis, M. Taki, and S. Pnevmatikos, Phys. Rev. **B38**, 11284 (1988).

[15] G. Rotoli, G. Costabile, and R. D. Parmentier, Phys. Rev. B41, 1958 (1990).

[16] G. Filatrella, G. Rotoli, N. Grønbech-Jensen, R. D. Parmentier, and N. F. Pedersen, J. Appl. Phys. 72, 3179 (1992).

[17] M. Cirillo, A. R. Bishop, P. S. Lomdahl, and S. Pace, J. Appl. Phys. 66, 1772 (1989).

[18] M. Cirillo, I. Modena, F. Santucci, P. Carelli, and R. Leoni, Physics Letters 167A, 175 (1992).

[19] K. C. Gupta, R. Garg, and I. J. Bahl, Microstip Lines and Slotlines, Artech House, Dedham, MA (1979).

[20] G. D. Alley, IEEE Trans. Microwave Theory and Techniques, MTT18, 1028 (1970).

[21] H. H. Li, J. Phys. Chem. Ref. Data, 9, 561 (1980).

[22] H. Schulze, R. Behr, F. Mueller, and J. Niemeyer, Appl. Phys. Lett. 73, 996 (1998).

## FIGURES

Figure 1 : The capacitively coupled Josephson junctions systems investigated in the paper. The dashed lines indicate shorting paths generating sub-circuits that we analyze before considering the whole system .

Figure 2 : (a) Current-voltage characteristics of a point Josephson junction pumped by the power emitted by a long Josephson junction biased on the first zero-field step ;(b) Dependence of the amplitude of the first Shapiro step shown in (a) upon the coupling parameter. Different symbols are relative to distinct bias points.

Figure 3 : (a) Current-voltage characteristic of one small junction pumped by two long junctions; (b) Dependence of the current amplitude of the highest Shapiro step in (a) upon the coupling parameter, for a fixed value of the bias current $\gamma = 0.3$ .

Figure 4 :(a) Current-voltage characteristic of a single small junction pumped by two coupled long junctions connected in series.

Figure 5 : (a),(b), and (c) Dependence of the amplitude of the first two Shapiro step shown in Fig. 4a upon the coupling parameter for three values of percentage length difference between the long junctions.

Figure 6 : (a) A photograph of the circuit that we have fabricated showing a basic building block similar to that of Fig. 1, i. e. two long junctions and two small junctions. The dark areas indicate the location of the junctions; (b) a sketch of the meander line nesting of the two arrays (each meander line represents the path of a series array). The line by side indicates the length of the unitary cell of our interdigital capacitor structure.

Figure 7 : Oscillators off (a) oscillator on (b) curves for an array of 64 small area junctions coupled to an array of 64 large area junctions. The horizontal (current) scale is $50\mu A/div$.

Figure 8 : Oscillator off (a) oscillator on (b) displays for two arrays each containing 8 junctions. The horizontal (current) scale is $50\mu A/div$.

Figure 9 : Oscillator off (a) oscillator on (b) traces for coupled arrays having each 1564 junctions. The horizontal (current) scale is $50\mu A/div$.

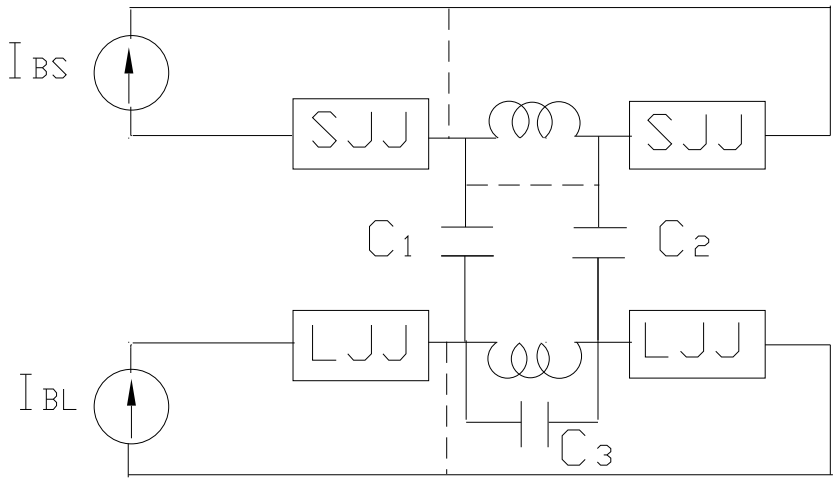
I BS
SJJ
SJJ
C1
C2
LJJ
LJJ
I BL
C3

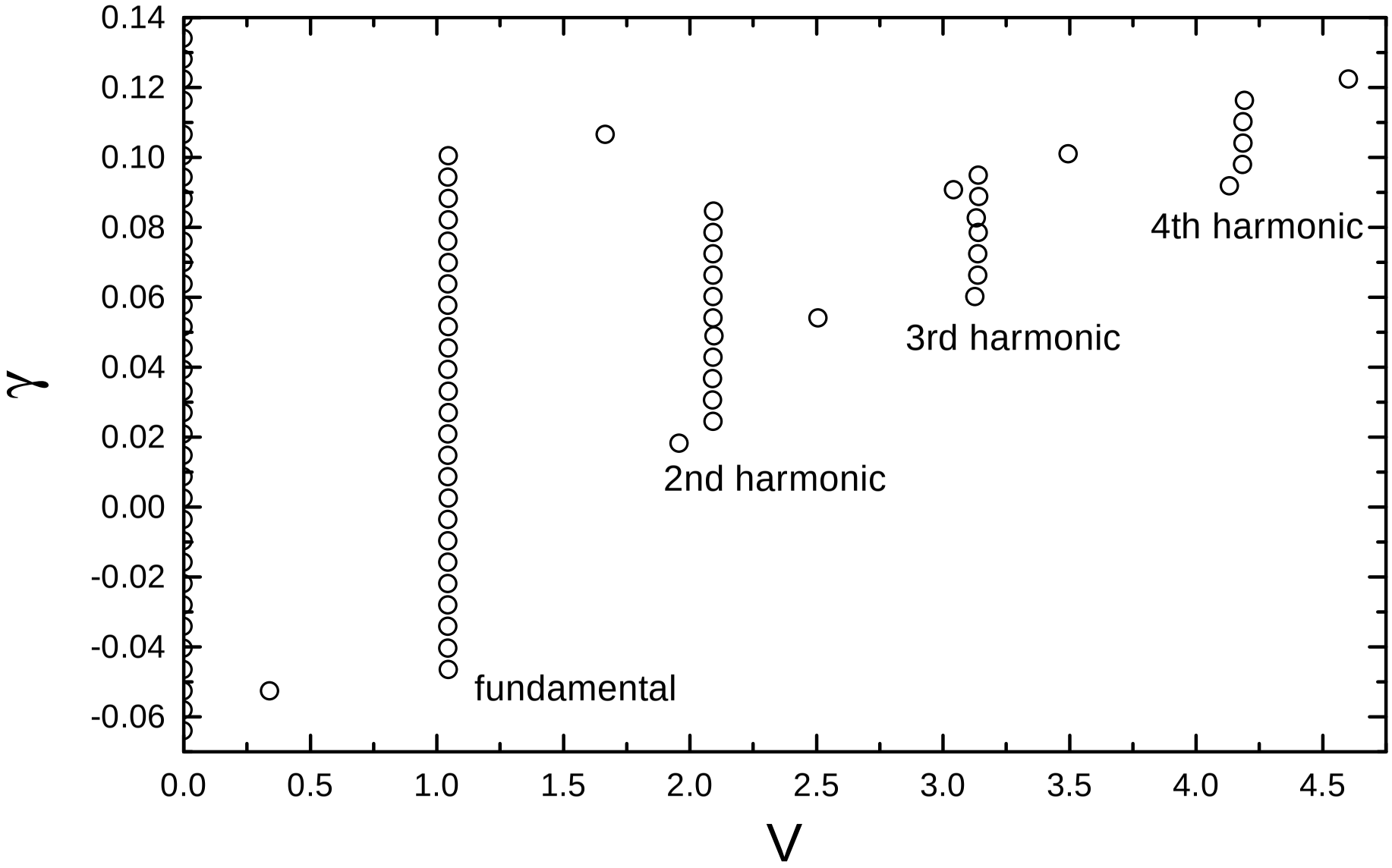
0.14
0.12
0.10
0.08
0.06
0.04
0.02
0.00
-0.02
-0.04
-0.06
γ
0.0
0.5
1.0
1.5
2.0
2.5
3.0
3.5
4.0
4.5
V
fundamental
2nd harmonic
3rd harmonic
4th harmonic

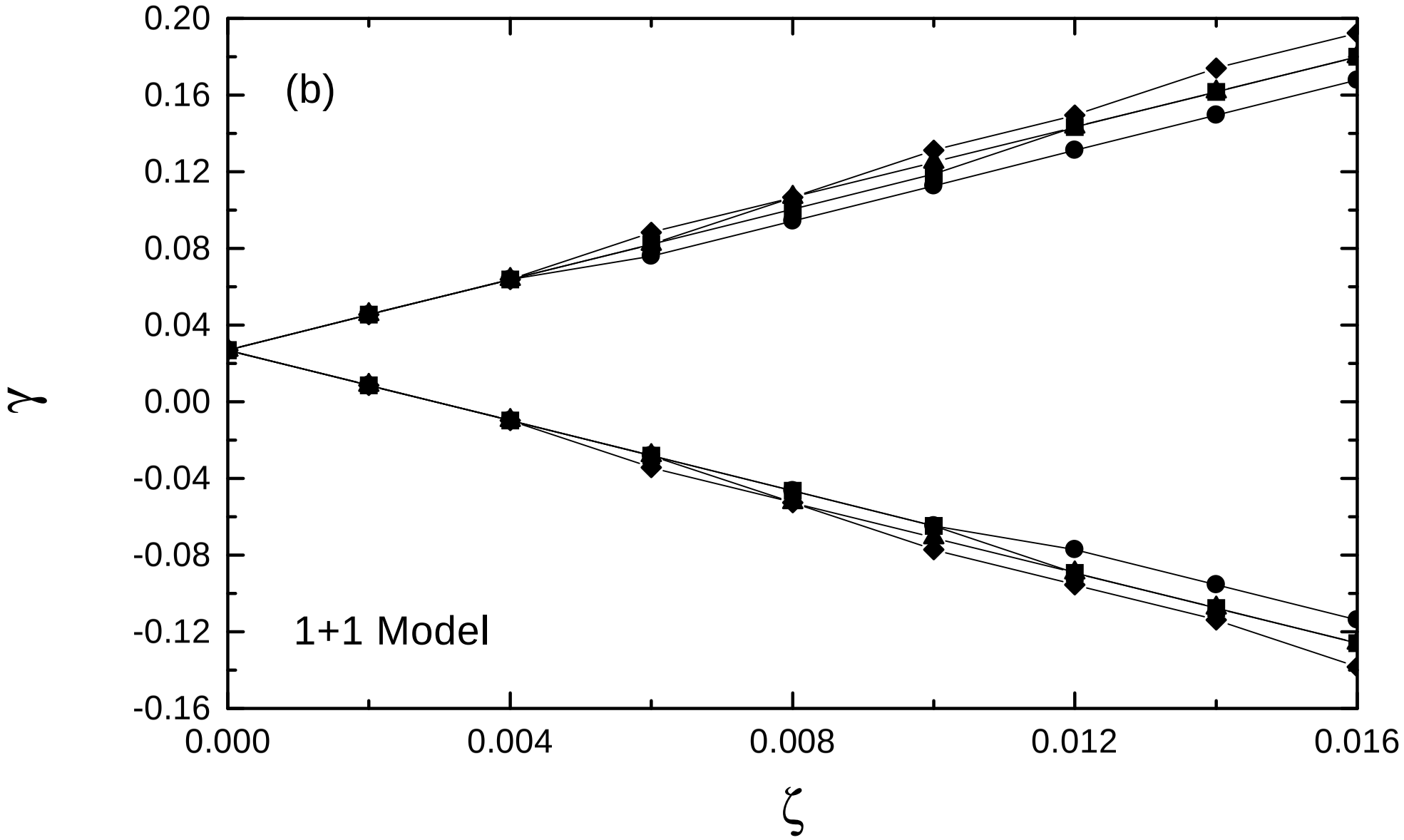
(b)
1+1 Model
0.20
0.16
0.12
0.08
0.04
0.00
-0.04
-0.08
-0.12
-0.16
0.000
0.004
0.008
0.012
0.016
γ
ζ

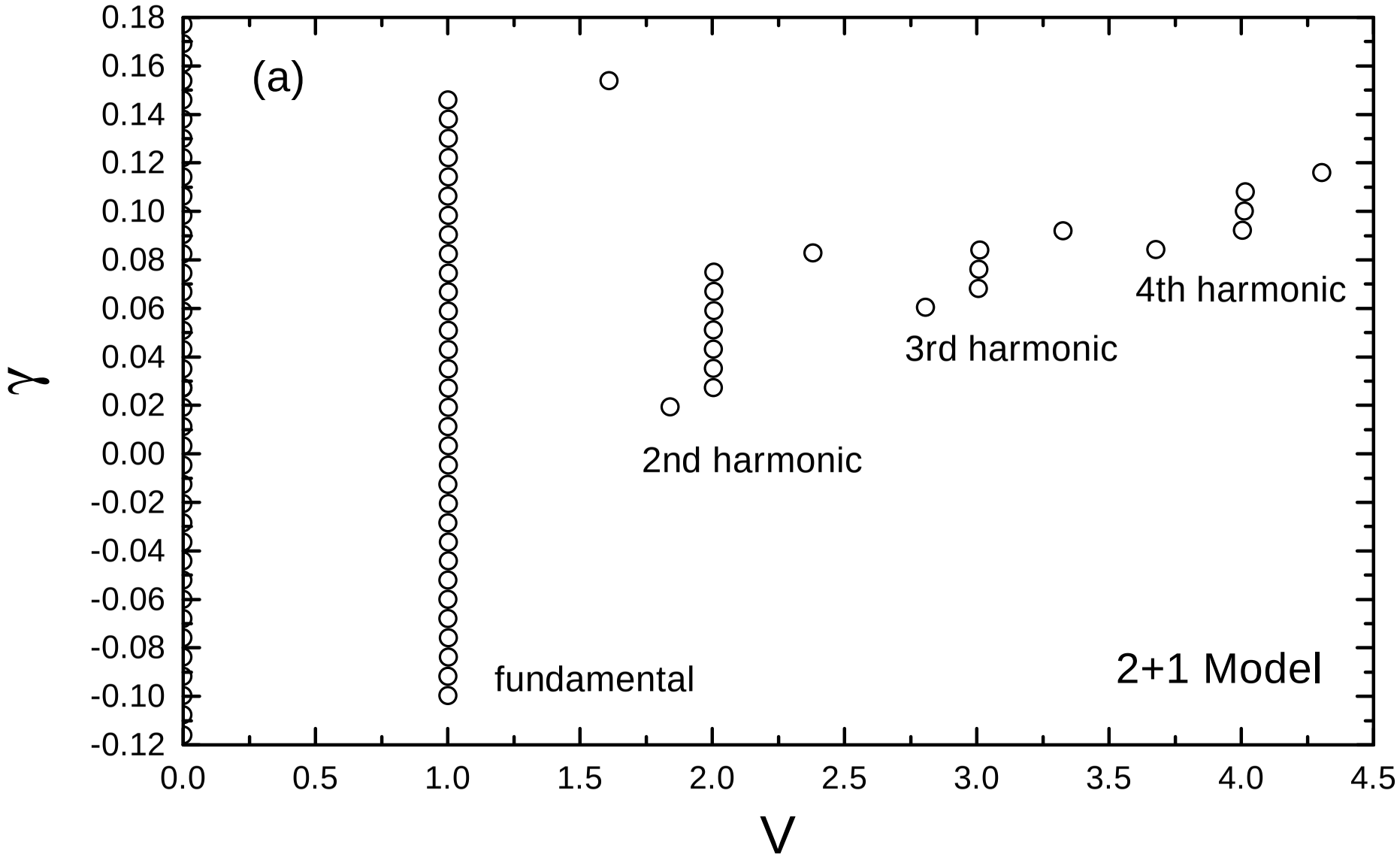
(a)
fundamental
2nd harmonic
3rd harmonic
4th harmonic
2+1 Model
γ
V
0.18
0.16
0.14
0.12
0.10
0.08
0.06
0.04
0.02
0.00
-0.02
-0.04
-0.06
-0.08
-0.10
-0.12
0.0
0.5
1.0
1.5
2.0
2.5
3.0
3.5
4.0
4.5

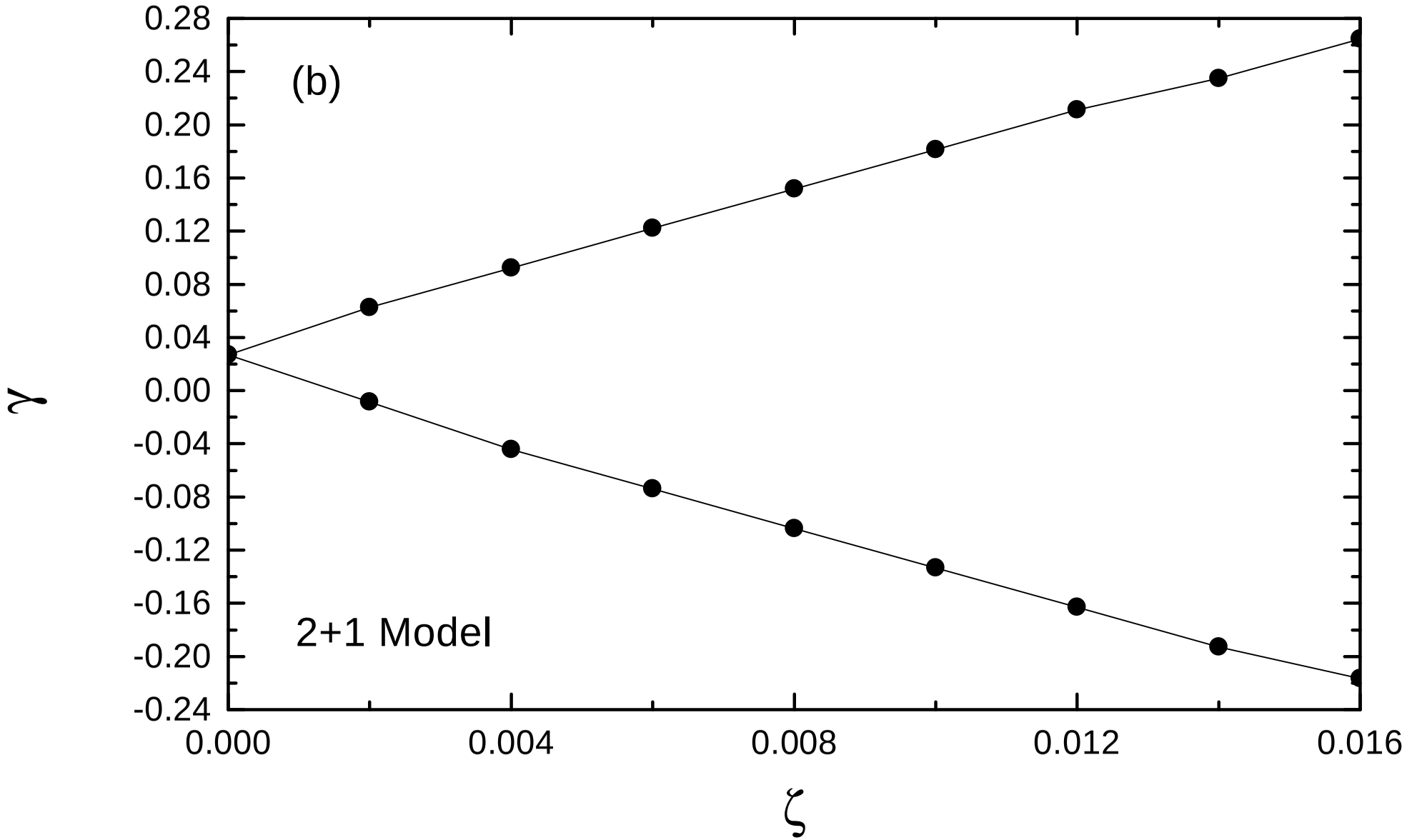
(b)
2+1 Model
0.28
0.24
0.20
0.16
0.12
0.08
0.04
0.00
-0.04
-0.08
-0.12
-0.16
-0.20
-0.24
0.000
0.004
0.008
0.012
0.016
γ
ζ

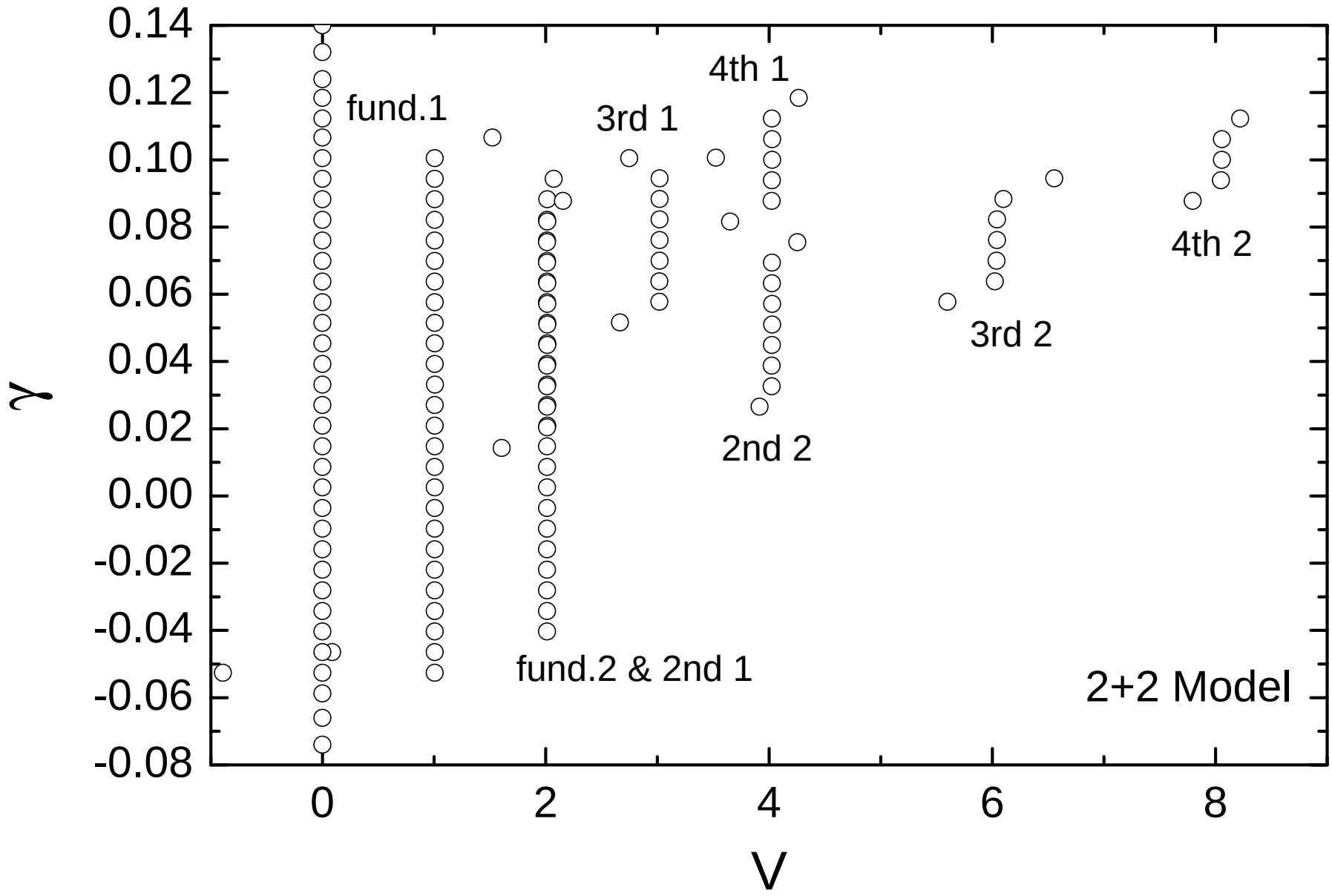
0.14
0.12
0.10
0.08
0.06
0.04
0.02
0.00
-0.02
-0.04
-0.06
-0.08
γ
0
2
4
6
8
V
fund.1
3rd 1
4th 1
2nd 2
3rd 2
4th 2
fund.2 & 2nd 1
2+2 Model

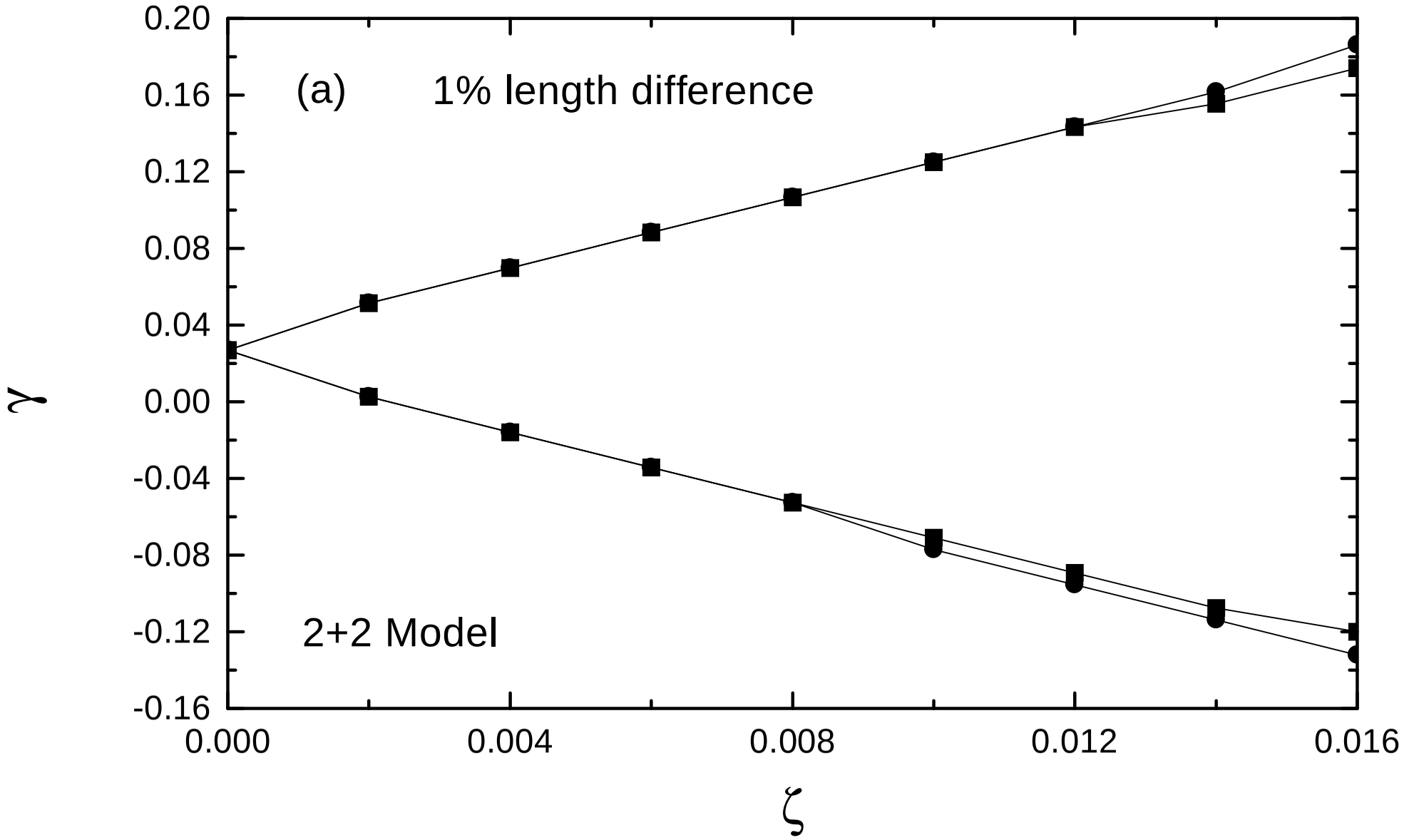
(a) 1% length difference
2+2 Model
0.20
0.16
0.12
0.08
0.04
0.00
-0.04
-0.08
-0.12
-0.16
0.000
0.004
0.008
0.012
0.016
γ
ζ

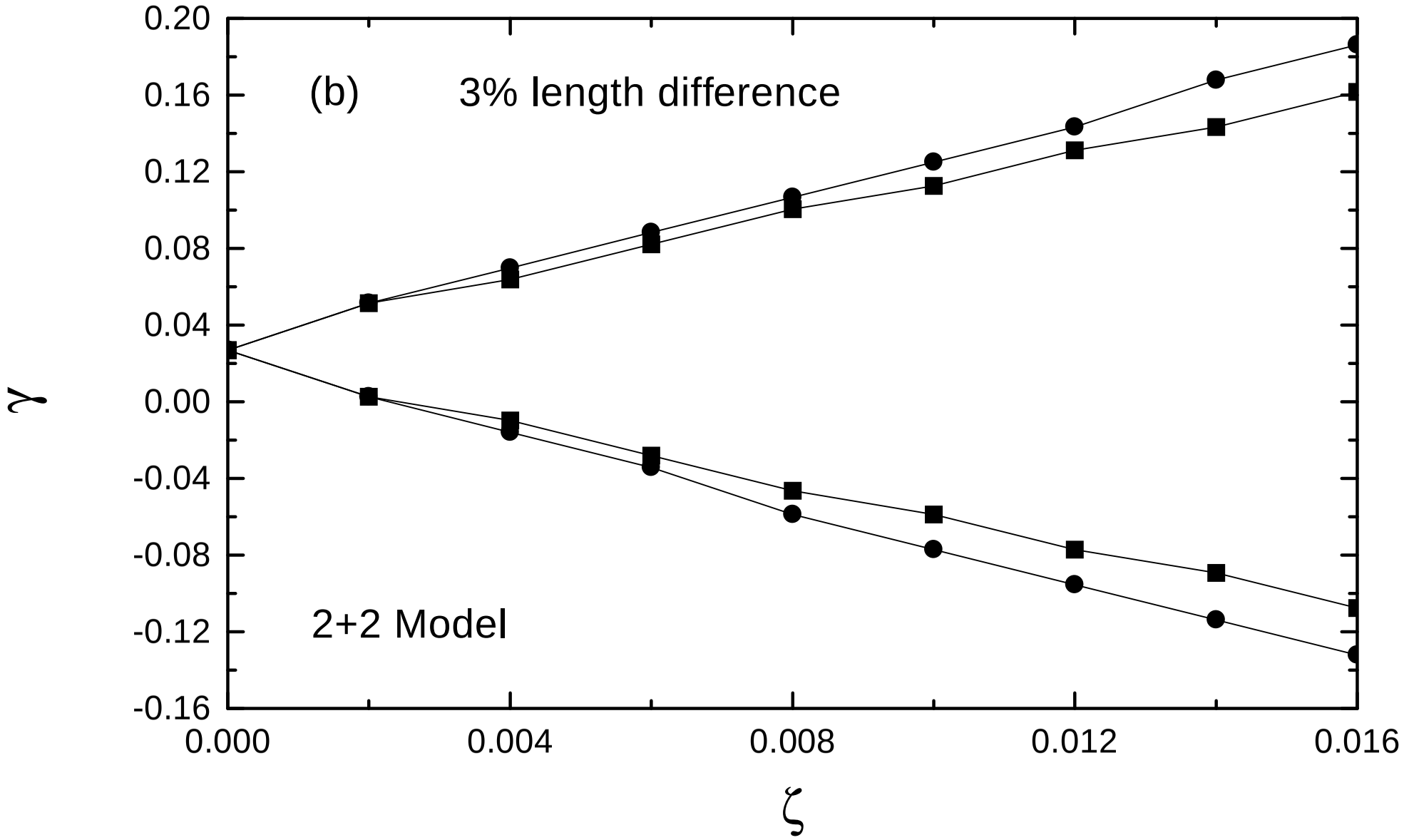
(b) 3% length difference
2+2 Model
0.20
0.16
0.12
0.08
0.04
0.00
-0.04
-0.08
-0.12
-0.16
0.000
0.004
0.008
0.012
0.016
γ
ζ

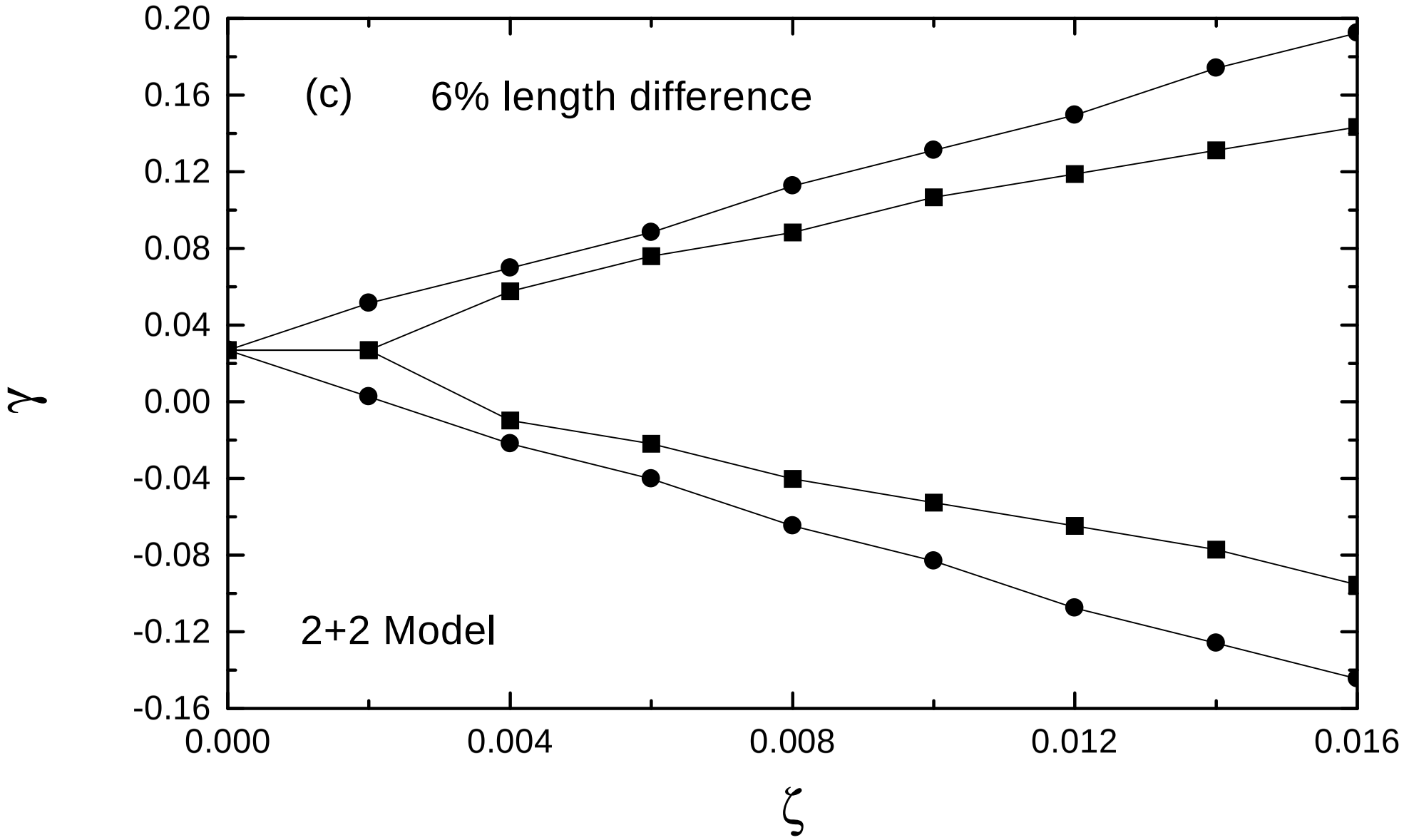
(c) 6% length difference
2+2 Model
0.20
0.16
0.12
0.08
0.04
0.00
-0.04
-0.08
-0.12
-0.16
0.000
0.004
0.008
0.012
0.016
γ
ζ

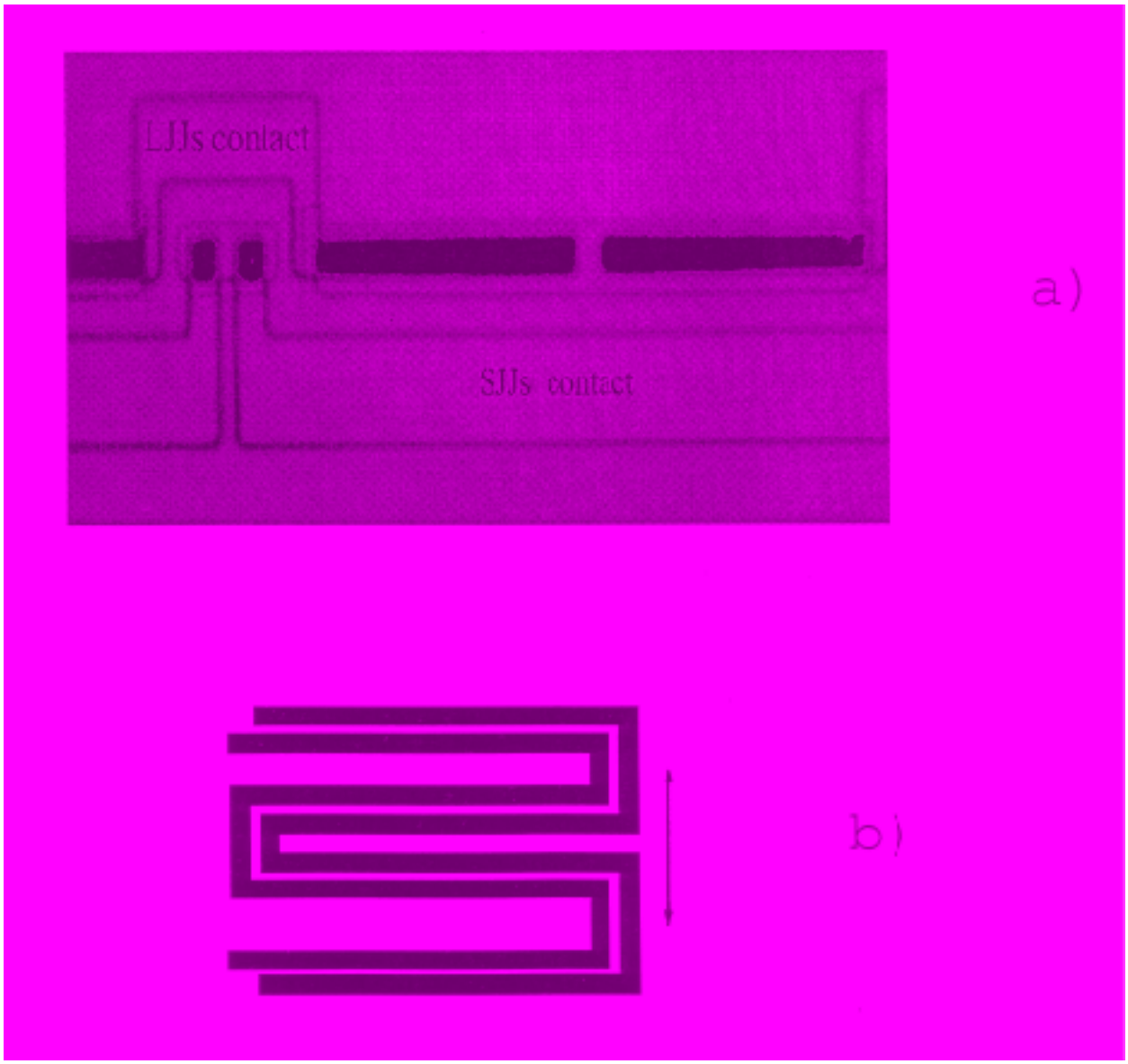
LJJs contact
SJJs contact
a)
b)

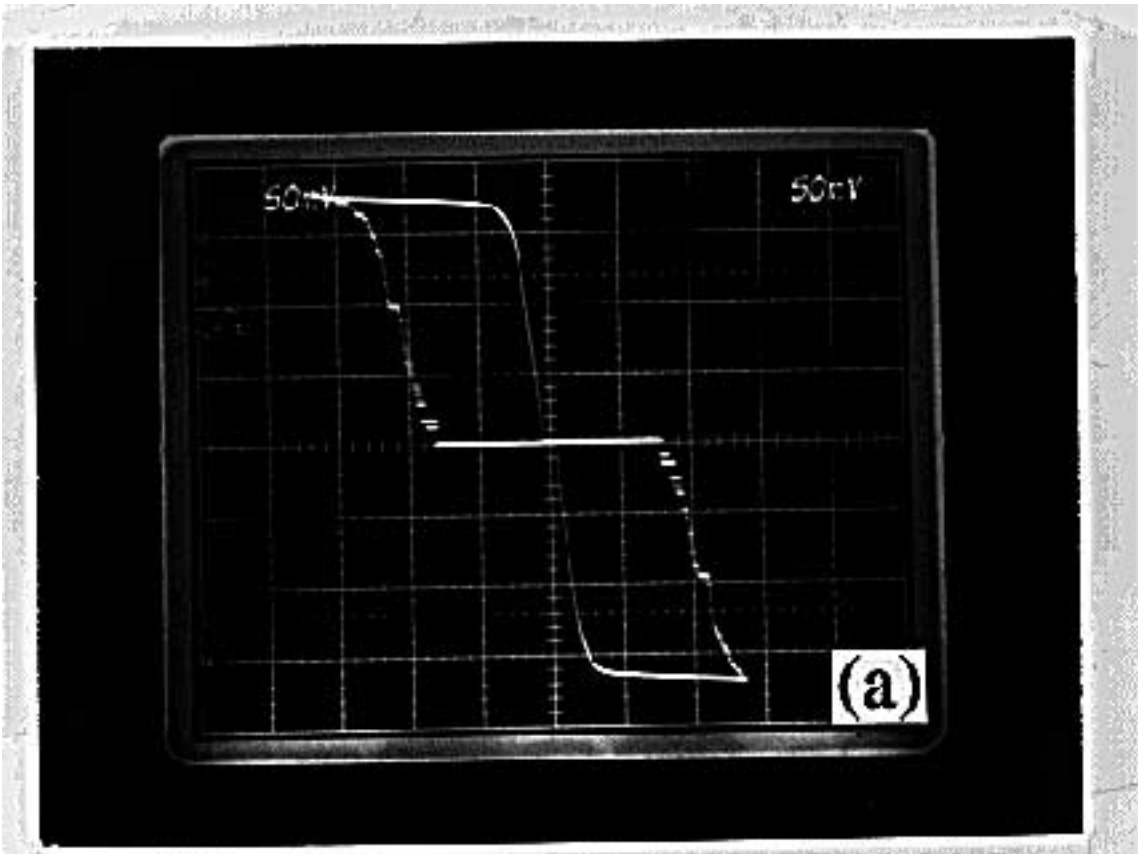
50mV
50mV
(a)

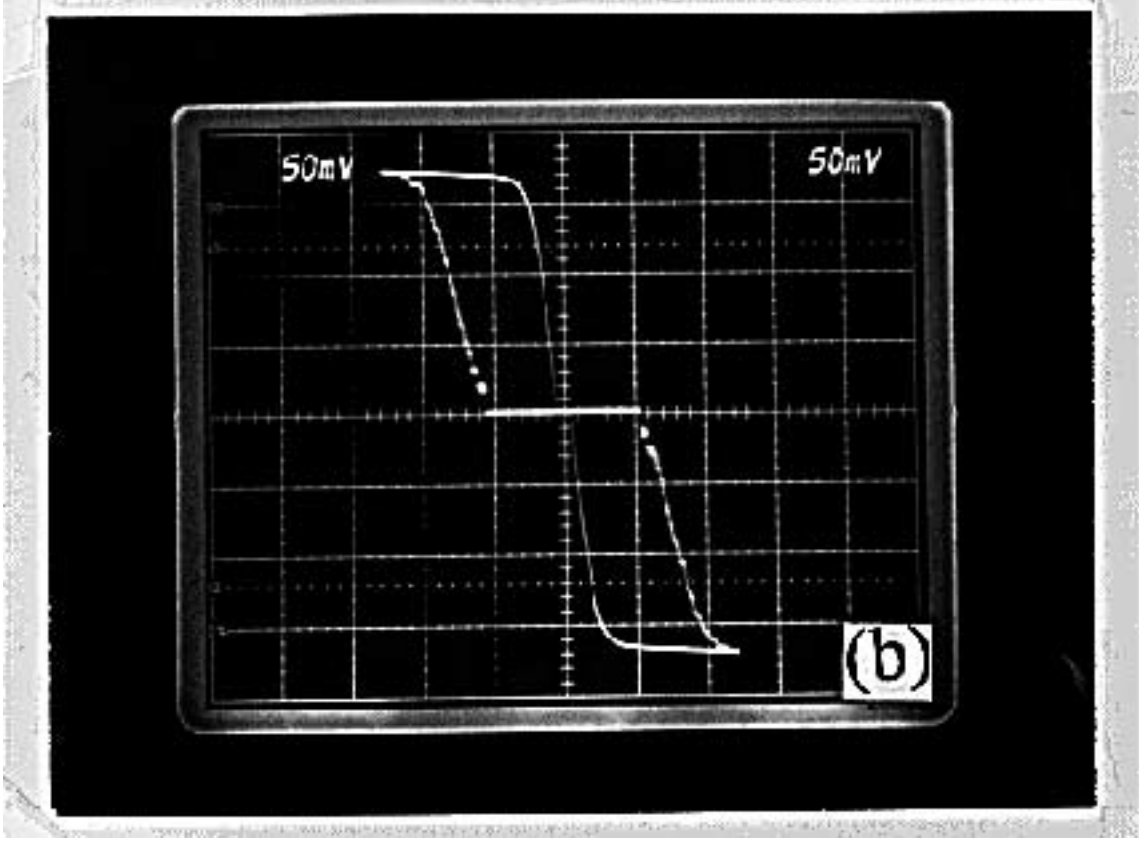
50mV
50mV
(b)

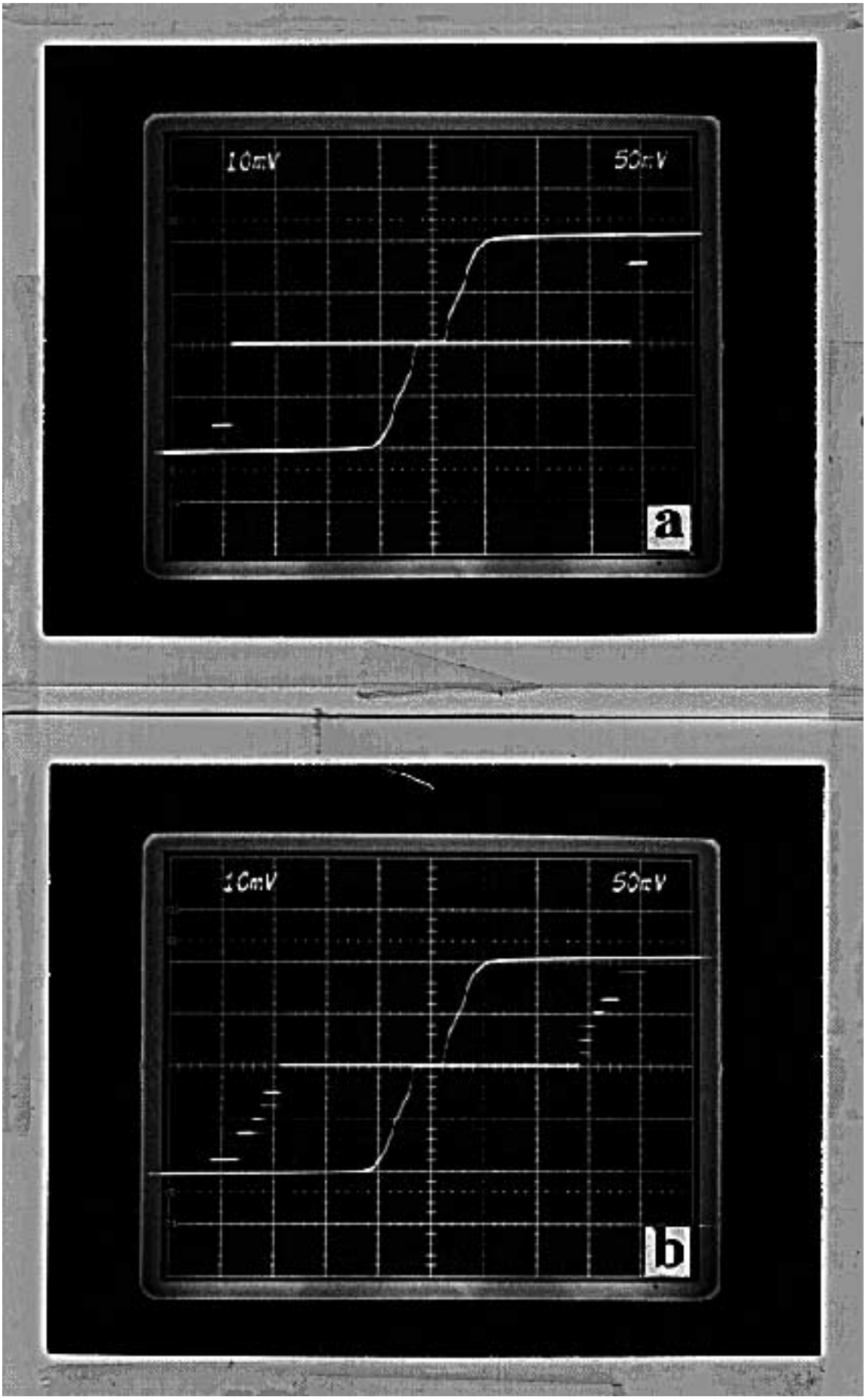
10mV
50mV
a
10mV
50mV
b

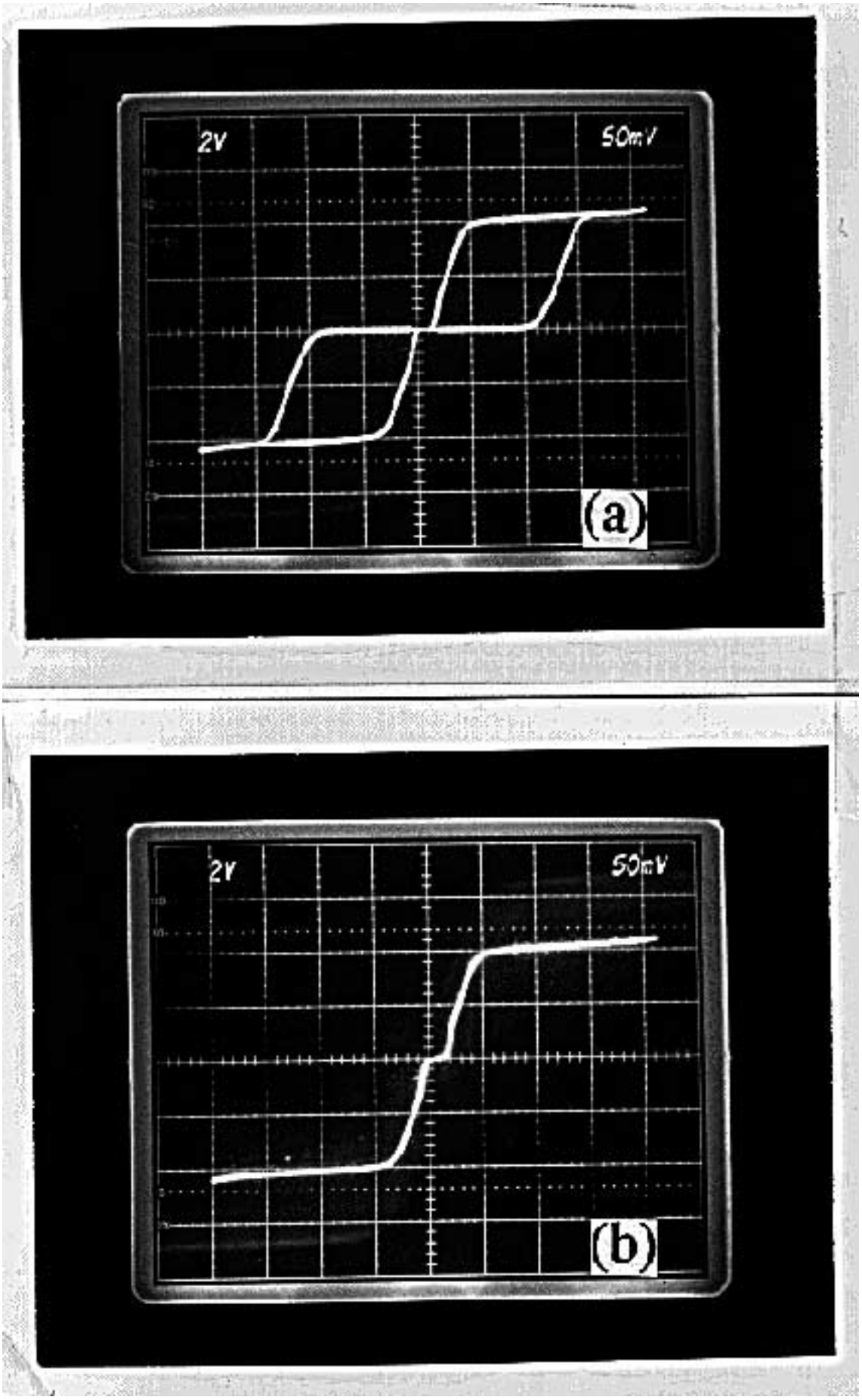
2V
50mV
(a)
2V
50mV
(b)